Journal of Applied Polymer Science

Size Effects of Cellulose Nanofibers for Enhancing the Crystallization of Poly(lactic acid)

Ryota Kose, Tetsuo Kondo
Graduate School of Bioresource and Bioenvironmental Sciences, Kyushu University, 6-10-1, Hakozaki, Higashi-Ku, Fukuoka 812-8581, Japan
Correspondence to: T. Kondo (E-mail: tekondo@agr.kyushu-u.ac.jp)

ABSTRACT: A desirable size of cellulose fibers for enhancing the crystallization of poly(lactic acid) (PLA) in composites was investigated by comparison among cellulose nanofibers with different widths on nanoscales. Namely, the crystallization behaviors of PLA in the presence of cellulose nanofibers were monitored with differential scanning calorimetry and polarized optical microscopy in terms of the crystallization rates of PLA. The smallest width of cellulose nanofibers was found to not necessarily provide better enhancement for the crystallization, presumably because of the preferential self-assembly of smaller cellulose nanofibers in PLA. Namely, when the width was smaller, the better effect expected for nanofibers did not appear in the composites. It is possible that an optimum width range of 60 nm, more or less, in the cellulose nanofibers may exist in balance between the favorable self-assembly as an enthalpy effect and the tendency toward dispersion as an entropy effect. © 2012 Wiley Periodicals, Inc. J. Appl. Polym. Sci. 128: 1200–1205, 2013

KEYWORDS: biofibers; nanocomposites; nanofiber; poly(lactic acid); crystallization

Received 4 March 2012; accepted 5 July 2012; published online 24 August 2012
DOI: 10.1002/app.38308

INTRODUCTION

Biodegradable polymeric composites with biomass fibers have been widely used in the construction and automobile industries.[1] Biomass fibers for reinforcement of plastics require characteristic advantages over synthetic ones: The fibers, of course, offer environmental benefits, namely, renewable under low energy production, and in addition, they are supposed to have a high specific strength and modulus with a low density. Among them, cellulose fillers having various widths have been developed to improve the properties of polymeric composites.[2,3]

Poly(lactic acid) (PLA) is well known as a biodegradable polymer. Because of its reasonable mechanical properties, PLA has been used in replacements of some common thermoplastics for packaging as films and fibrous materials.[4–7] Because glassy molded particles of PLA are provided by a quenching process of the melt state with a higher cooling rate, the heat resistance, such as heat distortion or the deflection temperature of the particles around 50–65°C, is not satisfactory for practical applications.[8,9] The acceleration of the crystallization rate for PLA during the practical process could possibility improve the heat resistance.[10]

Cellulose nanowhiskers in PLA composites have attracted attention for the improvement of the thermal and mechanical properties.[11–13] The size of the whiskers was estimated to be less than 10 nm in width and between 200 and 400 nm in length. However, it was still hard to achieve homogeneously dispersed whiskers in PLA without dispersing agents and surface modification; this limits practical use. Because the cellulose nanowhiskers have a very high surface area to encourage the formation of preferable aggregation, the mechanical properties of the PLA composites are supposed to be different, depending on the dispersion state of the nanowhiskers. Furthermore, cellulose nanocrystals were reported to exhibit a nucleating effect for PLA.[14] Therefore, there are two factors to be examined for the nucleating effect: the size and morphology of cellulose nanoobjects and the dispersion state.

Recently, we succeeded in preparing cellulose nanofibers with various morphologies and sizes on the nanoscale by aqueous counter collision (ACC) using the collision of a pair of high-speed water jets.[15] In particular, nanocellulose (NC)[16] prepared from microbial cellulose pellicles was supposed to provide further insight on the nanosize effects, such as the smaller, the better effect, by examination of the interaction in the composite with various plastics. Therefore, in this study, we dealt with the nucleating effect of NCs 18 to 57 nm in width by measuring the heat flows for the crystallization of PLA in the composites using differential scanning calorimetry (DSC) together with observation of the crystallization behavior.

EXPERIMENTAL

Materials

The following reagents were used as components for the Schramm & Hestrin (SH) culture medium: D-glucose, citric acid, and sodium hydroxide of a special grade were purchased from Wako Pure Chemical Industries, Ltd., Osaka, Japan. Disodium hydrogen phosphate heptahydrate of a special grade was purchased from Nacalai Tesque, Inc., Kyoto, Japan. Yeast extract and peptone were provided from Becton, Dickinson, and Co., NJ, USA.

PLA pellets were provided from Unitika Ltd., Osaka and Tokyo, Japan. Microfibrillated cellulose fibers (MFCs) 100 nm to 3 μm in width (Celish FD-100G) were provided by Daicel Chemical Industries Co., Ltd., Osaka and Tokyo, Japan. Microcrystalline cellulose (MCC) 11 $\pm$ 10 μm in width (FUNACEL II) was purchased from Funakoshi Co., Ltd., Tokyo, Japan.

Preparation of NC

Cellulose nanofibers as NC dispersed in water were prepared from microbial cellulose pellicles according to a previous article.[16] After inoculation into the SH culture medium[17] in a sterilized plastic container, *Gluconacetobacter xylinus* (formerly *Acetobacter xylinum*, ATCC53582) was cultured statically at 30°C to produce a gel-like membrane with a three-dimensional network structure of the secreted cellulose nanofibers; this was called a *microbial cellulose pellicle*. After 2 weeks of incubation, a pellicle about 1 cm in thickness was established covering the top of the culture medium. The pellicle was then washed with a 0.1% aqueous NaOH solution at about 80°C for 4 h and successively with water to remove protein, bacterial cells, and other residues. The purified pellicle was cut into cubes of about 1 cm^3 by a scissors before they were mixed with deionized water. The mixture containing 0.1% (w/w) cellulose was pretreated with a homogenizer (Physcotron NS-51, Microtec Co., Ltd., Chiba, Japan) for a few minutes at 20,000 rpm. The obtained suspension was provided for the subsequent treatment with an ACC system (Sugino MACHINE Ltd., Toyama, Japan) under 100 and 200 MPa ejecting pressures with 5 and 60 repetition times of the collision (= Pass) to disperse the cellulose nanofibers as NC into water.[15,16]

Transmission Electron Microscopy (TEM)

TEM images of the NC were employed for measurements of the fiber width. The aqueous dispersion containing about 0.01% cellulose nanofibers was sonicated with an ultrasonic apparatus for 10 s and mounted on copper grids before air drying. Then, the sample was negatively stained by aqueous 2% uranyl acetate and finally air-dried. The cellulose nanofibers on the grid were observed with a JEM-1010 (JEOL, Ltd., Tokyo, Japan) at an 80-kV accelerating voltage. The negative films of the acquired images were scanned to be digitized for measurements of the width for the individual cellulose nanofibers.

Preparation of PLA Composite Samples

At first, powdered PLA was prepared from the pellets in the following way: 50 g of PLA pellets was dissolved completely in 200 mL of chloroform. Then, a mixture of 200 mL of chloroform with 400 mL of methanol was added to the PLA/chloroform solution. The solvent was gradually removed from the solution under a reduced pressure with an evaporator at 40°C to obtain powdered PLA. Powders with a particle size smaller than 350 μm were collected with a suitable shifter. An average viscometric molecular weight of the collected PLA powders was 39,000.

One gram of the PLA powders was mixed with an aqueous suspension containing 0.01 g of the previously prepared cellulose nanofibers or the other individual agents of MFCs and MCC in a 50-mL Falcon tube. Deionized water was then added to the suspension with stirring to homogeneously mix PLA powder with cellulose nanofibers so that the total weight was 17 g. The mixture was rapidly frozen by liquid nitrogen before it was freeze-dried to finally provide compounded samples containing 1% (w/w) of the nucleating agent.

DSC

Isothermal crystallization was performed under a nitrogen atmosphere with a differential scanning calorimeter (Diamond DSC7, PerkinElmer Japan Co., Ltd., Kanagawa, Japan). After the instrument was calibrated with indium as a standard, sealed aluminum pans containing 5.0 $\pm$ 0.1 mg samples were placed. Samples were first heated to 200°C and maintained at this temperature for 10 min to completely eliminate the PLA crystalline resides. Then, it was quenched to 130°C at a rate of 200°C/min to keep samples at this temperature crystallized for 120 min. An isothermal temperature of 130°C was employed because of the practical uses for PLA in industries. During the process, the heat flow due to the crystallization of PLA in the samples was measured.

Polarized Optical Microscopy

To monitor the PLA crystallization process in samples, the following programmed procedure was carried out by DSC accompanied with polarized optical microscopy: 3.0 $\pm$ 0.1 mg of the individual sample was placed in a sealed aluminum pan for DSC. The sample pan was heated to 200°C, held for 10 min, then quenched to 130°C at a rate of 200°C/min to maintain the temperature for 3 and 10 min to crystallize the PLA in the samples, and finally quenched to 0°C at a rate of 200°C/min to hold for 10 min. In the case of the sample preparation without the crystallization, the sample in a pan was heated to 200°C, held for 10 min, quenched to 0°C at a rate of 200°C/min, and held there for 10 min. After the treated sample was picked up from the pan, it was observed with polarized optical microscopy (BHA, Olympus Co., Tokyo, Japan).

To observe the same position in a sample before and after the isothermal crystallization, the following procedures were conducted with a hot stage (FP82HT, Mettler-Toledo K.K., Tokyo, Japan). At first, the sample was heated to 200°C and cooled in water before it was observed under the polarized optical microscope. The same sample was also heated to 200°C, air-cooled to 130°C and maintained at this temperature for 3 min, then cooled in water, and observed. In this way, the positional relationship between the cellulose objects and the PLA crystals could be investigated.

RESULTS AND DISCUSSION

Differences in the Size and Morphology of the Cellulose Nanofibers

As reported previously,[16] the network structure of the nanofibers in the pellicle was visible by polarized optical microscopy after homogenization [Figure 1(a)]. The network of NC1, which was treated by the weaker ACC treatment [100 MPa, 5 passes, Figure 1(a)], was still slightly observed by polarized optical

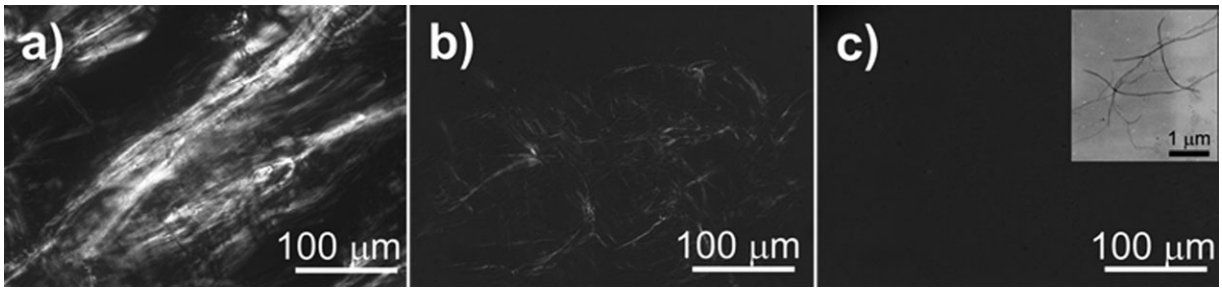

Figure 1. Polarized optical microscopic images of (a) homogenized cellulose nanofibers and (b) NC1 and (c) NC2 nanofibers, respectively. The inset in part c is a TEM image of the cellulose nanofibers.

microscopy; this indicated that the smaller fibers out of the microscopic range were dominant after preparation. After the stronger ACC treatment, these were no longer observed with a polarized optical microscope, but instead, fibers having nanosized widths (NC2) were observed by TEM, as shown in the inset of Figure 1(c). The cellulose nanofibers of NC2 exhibited a larger specific surface area of 55.9 m^2/g compared to that of MCC (1.3 m^2/g).[16] Namely, the surface area of NC2 was much larger, more than 40 times larger, than that of MCC. The widths of the cellulose nanofibers (NF, NC1, and NC2) thus treated are listed in the left column of Table I. NF, NC1, and NC2, as shown in Table I, indicate three kinds of cellulose nanofibers in width toward the smaller, which were prepared by the homogenizer, ACC under 100 MPa with 5 passes and under 200 MPa with 60 passes, respectively.

Enhancing the Crystallization Behaviors of PLA by Cellulose Nanofibers

Figure 2 shows the DSC thermogram of a heat flow of pure PLA during isothermal crystallization at 130°C. The crystallization of pure PLA started at point A in the thermogram after a short period when the sample was equilibrated at the temperature. Point B was the maximum of the exothermic peak, where the isothermal crystallization time was defined as t_i. In general, a shorter t_i indicates a lager crystallization rate. The crystallization rate of pure PLA slowed down beyond point B, which was presumably because of impingements among adjacent spherulites interfering with the growth of the entire crystallite. Finally, the measurement was terminated when no more change in the heat flow was detected. Here, the onset and offset times are indicated as intersections of a baseline, with both tangents having positive and negative maximum slopes, respectively. Decreases in both the onset and offset times reflect the induction of a faster crystallization. In Figure 3, DSC thermograms are shown for PLA with the different cellulose fiber nucleating agents used in this study. The onset time, offset time, and t_i of the samples are also listed in Table I. In comparison between the microsized and nanosized cellulose fibers, the smaller, the better nanosize effect appeared to significantly enhance the crystallization of PLA (see NF, NC1, and NC2). Among the three nanosized cellulose fibers, NF exhibited the smallest onset and offset times for the PLA crystallization. It was noted that the asymmetrical shape of exothermic peaks appeared in the DSC thermograms of the PLA/cellulose nanofibers, which differed from the symmetrical shape of microsized cellulose samples. Namely, the faster crystallization of PLA in the early stage ranged from 0 to 1.5 min occurred in the PLA/nanosized cellulose fibers.

Furthermore, the crystallization behavior of PLA with nanosized cellulose fibers was examined at different isothermal crystallization temperatures, 120 and 140°C. Although the difference in the t_i between PLA/NF and PLA/NC2 was within 1 min under isothermal crystallization at 120°C, the difference in t_i was larger by about 10 min at 140°C. Therefore, the higher isothermal temperature was advantageous for more clearly elucidating the nucleation effect of nanosized cellulose fibers for PLA. Considering the difficulty in determining the onset, offset, and t_i of the samples due to too much slow crystallization of PLA at 140°C, the isothermal crystallization occurred at 130°C in this study.

The relative degree of crystallinity as a function of time $[X_c(t)]$ was calculated by the following equation:

$$X_c(t) = A_t/A_\infty \times 100 \quad (1)$$

where A is the exothermic area under the DSC thermograms and t is the isothermal crystallization time. A_t is the exothermic area from $t = A$ to $t = t$ at the desired point and A_∞ is the

Table I. Fiber Width of the Samples, Onset and Offset Times, and t_i Values from the Differential Scanning Calorimetric Thermograms

Sample	Fiber width	Onset time (min)	Offset time (min)	t_i (min)
PLA	—	3.9 ± 0.4	23.4 ± 1.0	13.4 ± 0.8
PLA/MCC	11 ± 10 μm	3.8 ± 1.3	23.3 ± 0.8	12.7 ± 1.8
PLA/MFC	100 nm to 3 μm	1.9 ± 0.2	19.9 ± 0.8	9.9 ± 0.3
PLA/NF	57 ± 22 nm	0.8 ± 0.0	3.5 ± 0.1	1.4 ± 0.0
PLA/NC1	35 ± 19 nm	1.1 ± 0.0	5.9 ± 0.4	2.1 ± 0.1
PLA/NC2	18 ± 9 nm	1.2 ± 0.0	14.3 ± 1.2	3.4 ± 1.2

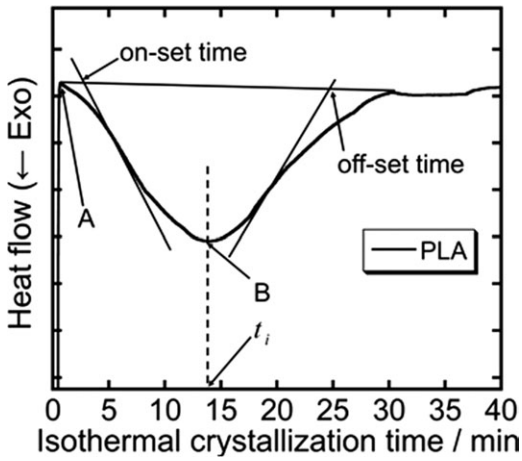

Figure 2. Differential scanning calorimetric thermogram of pure PLA undergoing an isothermal crystallization process at 130°C. Point A indicates the starting crystallization of PLA. The onset time and offset time are defined as intersections of a baseline with both tangents having a positive and negative maximum slope. Point B is the maximum of the exothermic peak.

total area surrounded by the thermograms and the baseline. The time at a relative crystallinity of 50% ($t_{1/2}$) is listed in the last column of Table II. The lower $t_{1/2}$ value was assumed as the higher crystallization rate. As the $t_{1/2}$ value of 2.7 for PLA/NF was about one-fifth of $t_{1/2}$ for PLA alone, the NF was supposed to accelerate the crystallization rate of PLA by five times. This case was the most effective among the cellulose nanofibers used in this study.

The growth type of crystallization could be estimated with the following Avrami equation:

$$X_c(t) = 1 - \exp(-Kt^n) \tag{2}$$

where $X_c(t)$ is the relative degree of crystallinity as a function of time, n is a constant depending on the mechanism of a crystal growth with nucleation, and K is the crystallization rate constant. Equation (2) can be transformed to eq. (3) as follows:

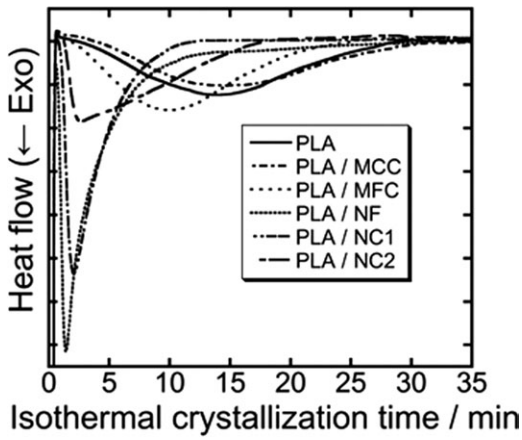

Figure 3. Differential scanning calorimetric thermogram of each sample responsible for the respective isothermal crystallization process at 130°C.

Table II. Avrami Parameters and $t_{1/2}$ Values

Sample	n	$-\ln K$ (min^{-n})	$t_{1/2}$ (min)
PLA	2.8 ± 0.1	7.8 ± 0.3	13.9 ± 0.2
PLA/MCC	2.6 ± 0.2	7.5 ± 0.6	14.5 ± 1.2
PLA/MFC	2.8 ± 0.1	7.2 ± 0.4	11.1 ± 0.7
PLA/NF	—	—	2.7 ± 0.1
PLA/NC1	—	—	3.4 ± 0.1
PLA/NC2	—	—	7.3 ± 0.6

$$\ln[-\ln(1 - X_c(t)] = \ln K + n \ \ln \ t \tag{3}$$

When $\ln[-\ln(1 - X_c(t))]$ is plotted as a function of $\ln t$ in the range from the onset time to the offset time (Figure 4), n and $\ln K$ can be obtained from the slope and the intercept, respectively. The n values, because of the liner relationship for PLA, PLA/MCC, and PLA/MFC, were around 2.6–2.8; this suggested a three-dimensional crystallization growth and homogeneous nucleation mechanism.[14,18–21]

When the single Avrami exponent (n) is provided, it indicates that a single mechanism governed the crystallization process.[19,21] In this case, a relationship between $\ln[-\ln[1 - X_c(t)]]$ and $\ln t$ had to be a linear, as shown in the PLA/microsized cellulose fibers of Figure 4. However, the PLA/cellulose nanofibers with NF, NC1, and NC2 did not exhibit such a linear relationship, as shown in Figure 4. Therefore, the crystallization behavior in the PLA/the cellulose nanofibers was not assumed as a single mechanism; this was different from the microsized cellulose samples of MFC and MCC. Furthermore, the slope (n) of PLA with cellulose nanofibers in the early stage of the isothermal crystallization was larger than those of PLA and PLA with microsized cellulose fibers. It was reported that the n values of a crystallization mode for heterogeneous nucleation were in the range from 3.5 to 5.[14,22] Therefore, a heterogeneous crystallization of PLA occurred in PLA with nanosized cellulose at the early stage of the isothermal crystallization.

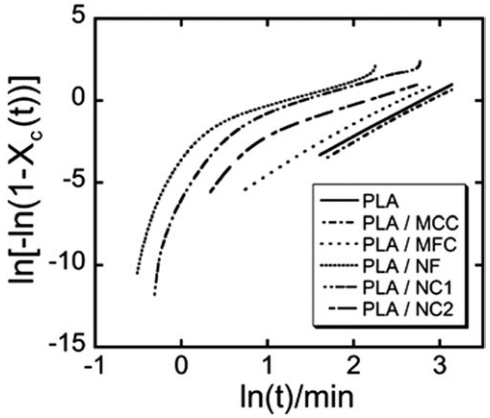

Figure 4. Plot of $\ln[-\ln[1 - X_c(t)]]$ versus $\ln(t)$ obtained from the differential scanning calorimetric thermograms at 130°C to calculate the Avrami exponent.

Applied Polymer SCIENCE

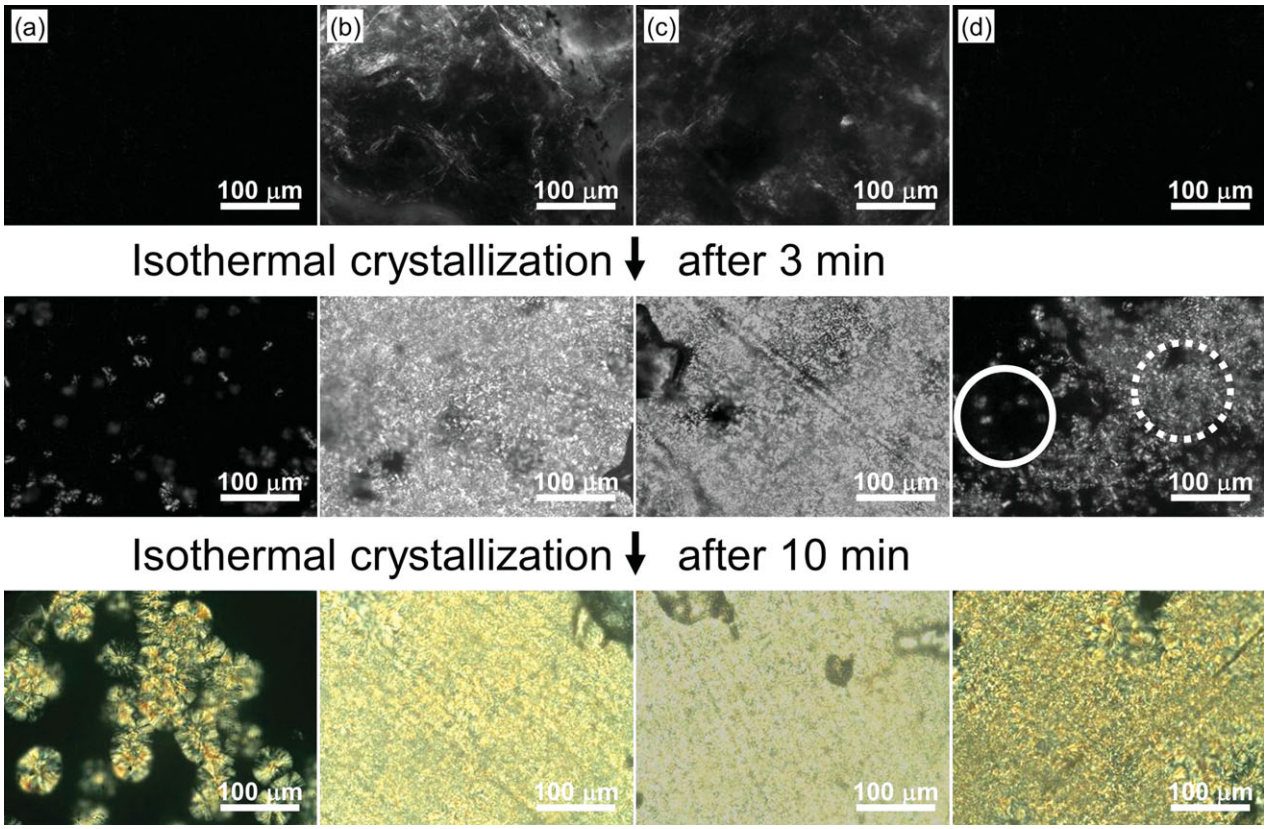

Figure 5. Polarized optical microscopic images of the microcrystals of PLA in (a) pure PLA, (b) PLA/NF, (c) PLA/NC1, and (d) PLA/NC2 before and after the isothermal crystallization for 3 and 10 min at 130°C. (d) Two areas surrounded by solid and dotted lines in PLA/NC2 after the isothermal crystallization indicating the empty and occupied parts of the microcrystals in the sample. [Color figure can be viewed in the online issue, which is available at wileyonlinelibrary.com.]

The distributions of PLA crystals in the composites with NF (ca. 57 nm in width), NC1 (ca. 35 nm in width), and NC2 (ca. 18 nm in width) were individually observed before and after isothermal crystallization at 130°C for 3 and 10 min under a polarized optical microscope, as shown in Figure 5. Microcrystals of PLA appeared densely for all of the systems from b to d in the figure after isothermal crystallizations at 130°C for 10 min. However, the microcrystals of PLA in PLA/NC2 appeared sparsely compared with those in PLA/NF and NC1 after 3 min of isothermal crystallization. The microcrystals of PLA in PLA/NC2 were located in two distinguishable areas, an empty area and an occupied area; these are surrounded by solid and dotted lines in Figure 5(d) and occurred after 3 min of isothermal crystallization. These results indicate that smaller fibers, on the nanoscale, were not necessarily better for inducing the crystallization of PLA.

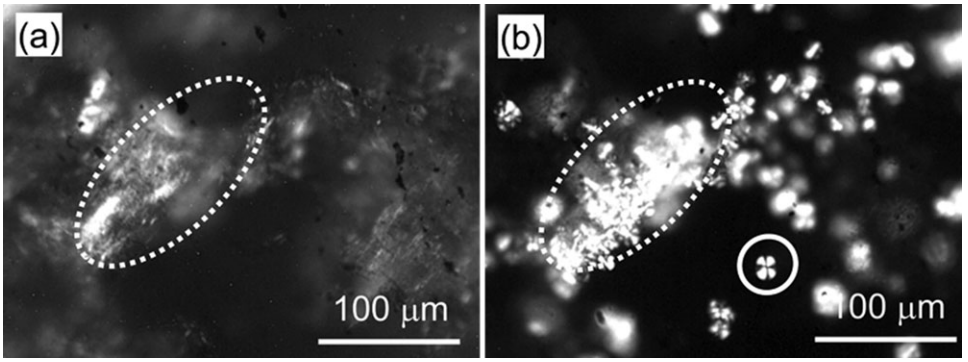

Figure 6. Polarized optical microscopic images showing the relationship between the distribution of NC2 and the microcrystals of PLA in PLA/NC2 (a) before and (b) after isothermal crystallization. The areas surrounded by the dotted line are the same positions in PLA/NC2 before and after the isothermal crystallization. The PLA spherulite is surrounded by a solid line after the crystallization.

In a comparison of the same area before and after isothermal crystallization at 130°C in the PLA/NC2 sample, both the distribution of the individual NC and the growth of PLA microcrystals were investigated. Before isothermal crystallization, as shown in Figure 6(a), aggregates of NC2 were observed as an area with a weaker light intensity under cross Nicole in a polarized optical microscope. After isothermal crystallization, the highly bright area was found to be at the same position where the aggregate of NC2 had already existed, as surrounded by the dotted line in Figure 6(b). In addition, PLA spherulites alone with a higher brightness were also observed in the circular area surrounded by the solid line [see Figure 6(b)]. This behavior indicated that NC2 induced nucleation of PLA on the fiber surface as a scaffold. Both the self-aggregation and the interfacial interaction of the smallest NC2 were supposed to be more favorable than those of the larger nanosized NC1 and NF; this strongly interfered with the homogeneous distribution of NC2 in the presence of PLA. In this way, the smaller size of the cellulose fibers on nanoscales did not necessarily provide an optimistic factor for enhancing the crystallization of PLA. Rather, the distribution of nanofibers in the system was a more influential factor.

It was noted that two phenomena, the homogeneous and heterogeneous crystallizations, occurred simultaneously in PLA/NC2. In general, either a homogeneous or a heterogeneous crystallization was dominant for PLA crystallization in the PLA composites.[19,22] This phenomenon in PLA/NC2 indicated that a number of PLA crystals occurred in the NC2 aggregates; in other words, the NC2 aggregate consisting of cellulose nanofibers was an effective nucleating agent for PLA. This characteristic of highly inducing crystallization on the surface of NC2 aggregate would make it possible by the composition to design a PLA material with a desired crystallinity.

The crystallization behavior of PLA and PLA with NF or NC2 was investigated under cooling scans from the melting temperature to room temperature. PLA with NF or NC2 was crystallized to achieve more than 10% crystallinity between the glass-transition and melting temperatures during the cooling process from the melted state at a rate of 10°C/min, although PLA alone was not crystallized in the scanning range. We believe that a slower cooling rate increased the crystallinity of PLA by enhancing the cellulose nanofibers.

CONCLUSIONS

In this study, cellulose nanofibers with various sizes on the microscale and nanoscale were compared in terms of inducing the crystallization of PLA with DSC analyses and polarized optical microscopy.

In a comparison of PLA crystallization rates in composites with cellulose, the nanofibers were more effective as a nucleation agent than microsized cellulose fibers. The crystallization behavior of PLA in the presence of cellulose nanofibers was not assumed as a single mechanism, presumably because of the heterogeneous dispersion of the nanofibers in the PLA composites. In particular, NC2 with the smaller width was found to exhibit the lowest effect among the three nucleation agents of the cellulose nanofibers. This may have been due to the preferable self-aggregation of NC2 in the PLA composites. Therefore, the smaller size of cellulose nanofibers on the nanoscale does not necessarily make a better nucleating agent for PLA. This nanosize effect was not like the smaller, the better effect that is believed to exist in general. On the contrary, PLA crystallization in the presence of NF 60 nm in width was superior to other systems with cellulose nanofibers. Furthermore, the network formation of nanofibers may also be an important factor in PLA crystallites.

REFERENCES

1. Netravali, A. N.; Chabba, S. *Mater. Today* **2003,** *6*, 22.
2. Eichhorn, S. J.; Dufresne, A.; Aranguren, M.; Marcovich, N. E.; Capadona, J. R.; Rowan, S. J.; Weder, C.; Thielemans, W.; Roman, M.; Renneckar, S.; Gindl, W.; Veigel, S.; Keckes, J.; Yano, H.; Abe, K.; Nogi, M.; Nakagaito, A. N.; Mangalam, A.; Simonsen, J.; Benight, A. S.; Bismarck, A.; Berglund, L. A.; Peijs, T. *J. Mater. Sci.* **2010,** *45*, 1.
3. Nakagaito, A. N.; Yano, H. *Appl. Phys. A* **2005,** *80*, 155.
4. Auras, R.; Harte, B.; Selke, S. *Macromol. Biosci.* **2004,** *4*, 835.
5. Drumright, R. E.; Gruber, P. R.; Henton, D. E. *Adv. Mater.* **2000,** *12*, 1841.
6. Sinclair, R. G. *J. Macromol. Sci. A* **1996,** *33*, 585.
7. Lunt, J. *Polym. Degrad. Stab.* **1998,** *59*, 145.
8. Wang, Y.; Gómez Ribelles, J. L.; Salmerón Sánchez, M.; Mano, J. F. *Macromolecules* **2005,** *38*, 4712.
9. Kalb, B.; Pennings, A. *J. Polymer* **1980,** *21*, 607.
10. Harris, A. M.; Lee, E. C. *J. Appl. Polym. Sci.* **2008,** *107*, 2246.
11. Petersson, L.; Kvien, I.; Oksman, K. *Compos. Sci. Technol.* **2007,** *67*, 2535.
12. Oksman, K.; Mathew, A. P.; Bondeson, D.; Kvien, I. *Compos. Sci. Technol.* **2006,** *66*, 2776.
13. Bondeson, D.; Oksman, K. *Compos. A* **2007,** *38*, 2486.
14. Pei, A.; Zhou, Q.; Berglund, L. A. *Compos. Sci. Technol.* **2010,** *70*, 815.
15. Kondo, T.; Morita, M.; Hayakawa, K.; Onda, Y. U. S. Pat. 7,357,339 (**2008**).
16. Kose, R.; Mitani, I.; Kasai, W.; Kondo, T. *Biomacromolecules* **2011,** *12*, 716.
17. Hestrin, S.; Schramm, M. *Biochem. J* **1954,** *58*, 345.
18. Krikorian, V.; Pochan, D. *J. Macromolecules* **2004,** *37*, 6480.
19. Lin.Y.; Zhang.K.-Y.; Dong, Z.-M.; Dong, L.-S.; Li, Y.-S. *Macromolecules* **2007,** *40*, 6257.
20. Tsuji, H.; Takai, H.; Saha, S. K. *Polymer* **2006,** *47*, 3826.
21. Iannace, S.; Nicolais, L. *J. Appl. Polym. Sci.* **1997,** *64*, 911.
22. Liao, R.; Yang, B.; Yu, W.; Zhou, C. *J. Appl. Polym. Sci.* **2007,** *104*, 310.